Cerebral Cortex August 2012;22:1786–1798
doi:10.1093/cercor/bhr275
Advance Access publication September 27, 2011

D4 Dopamine Receptors Modulate NR2B NMDA Receptors and LTP in Stratum Oriens of Hippocampal CA1

Marina Herwerth[1], Vidar Jensen[2], Martin Novak[3], Witold Konopka[3], Oivind Hvalby[2] and Georg Köhr[1]

[1]Department of Molecular Neurobiology, Max-Planck-Institute for Medical Research, D-69120 Heidelberg, Germany, [2]Department of Physiology, Institute of Basic Medical Science, University of Oslo, N-0317 Oslo, Norway and [3]Molecular Biology of the Cell I, German Cancer Research Center (DKFZ), D-69120 Heidelberg, Germany

Address correspondence to G. Köhr, Department of Molecular Neurobiology, Max-Planck-Institute for Medical Research, Jahnstrasse 29, D-69120 Heidelberg, Germany. Email: kohr@mpimf-heidelberg.mpg.de.

Dopamine plays an important role in synaptic plasticity and learning and is involved in the pathogenesis of various neurological and psychiatric disorders. Here, we reveal staining of dopaminergic fibers in stratum oriens of the mouse hippocampal CA1 region, a finding that is consistent with earlier reports. Furthermore, we examined the effect of dopamine agonists on NMDAR-dependent early long-term potentiation (LTP) (40 min) during γ-aminobutyric acid $(GABA)_A$-mediated blockade. LTP of the AMPA component was strongly reduced in stratum oriens but barely affected in stratum radiatum. This layer-specific effect was caused by D4 receptor activation, which augmented the inactivation of synaptic NMDAR-mediated currents (NMDA EPSCs) during LTP induction through a Ca^{2+}-dependent G-protein–independent mechanism. A similar dopaminergic modulation of both NMDA EPSCs and LTP was also observed in mice constitutively lacking NR2A but was absent in mice lacking NR2B in principal forebrain neurons. Together, these experiments strongly indicate that dopaminergic modulation of early LTP in stratum oriens occurs through NMDARs containing NR2B subunits via D4Rs. Thus, a dopamine hyperfunction in stratum oriens may result in NMDAR hypofunction that could affect both normal and pathological conditions.

Keywords: L-745,870, PD168077, schizophrenia, SKF38393, stratum radiatum

Introduction

The dopamine system is thought to play an important role in hippocampus-mediated learning and memory (Lisman and Grace 2005; O'Carroll et al. 2006) and seems also highly relevant to the pathogenesis of several psychiatric disorders including attention-deficit/hyperactivity disorder (ADHD) and schizophrenia (Lewis and Lieberman 2000; Winterer and Weinberger 2004). The hippocampal manifestation of schizophrenia may be characterized by dysfunctions of 2 neurotransmitter pathways: a dopamine (DA) hyperfunction caused by an increased firing rate of dopaminergic neurons localized to the ventral tegmental area (VTA) and an NMDA hypofunction of the glutamatergic system (reviewed in Lisman et al. 2008). The NMDA hypofunction appears to comprise the main features of schizophrenia: positive symptoms like hallucinations, negative symptoms like social withdrawal and cognitive defects including deficits in association and working memory (Greene 2001). The characterization of the functional link between the dopaminergic and the glutamatergic systems in the hippocampus is still incomplete.

The VTA and the substantia nigra supply the hippocampal formation with dopaminergic fibers. These fibers are mainly localized in the subiculum, hilus, and the stratum lacunosum-moleculare (SLM) (Gasbarri et al. 1997). This dopaminergic innervation could modulate glutamatergic synaptic transmission and synaptic plasticity within the hippocampal CA1 region through both D1-like and D2-like receptor families (Tarazi and Baldessarini 2000). Electrophysiological recordings performed in distinct CA1 layers have demonstrated a dopaminergic modulation of the direct cortical pathway to CA1 in SLM with a possible contribution from the inhibitory network (Otmakhova and Lisman 1999; Romo-Parra et al. 2005; Ito and Schuman 2007). At the Schaffer collateral–commissural synapses in stratum radiatum (RAD), the application of DA agonists or antagonists have indicated that D1-like receptors (D1R, D5R) increase the magnitude of early long-term potentiation (LTP) (Otmakhova and Lisman 1996) and stabilize late LTP both in vitro (Frey et al. 1991; Huang and Kandel 1995) and in vivo (Swanson-Park et al. 1999; Lemon and Mnahan-Vaughan 2006). Furthermore, selective genetic inactivation of the D1R suggested that D1Rs but not D5Rs are critical for both LTP at CA1 synapses and spatial learning (Granado et al. 2008; Ortiz et al. 2010). In contrast, the effects of D2-like receptors (D2R, D3R, D4R) are less explored in CA3-to-CA1 synapses and observations are still inconclusive. A D3R agonist has been shown to enhance LTP (Swant and Wagner 2006), whereas D3R mutant mice exhibited normal learning abilities (Xing et al. 2010). Notably, a D4R agonist depotentiated LTP in response to neuregulin-1 and theta-patterned stimuli (Kwon et al. 2008). Most studies have investigated the dopaminergic modulation of synaptic transmission and synaptic plasticity in CA1 with intact inhibition, which precluded an attribution of dopamine-mediated effects to either glutamatergic or γ-aminobutyric acid (GABA)ergic synapses. Moreover, very few studies have examined the dopaminergic modulation in stratum oriens (OR), in spite of the anatomical evidence for a stronger dopaminergic innervation of OR than RAD (Verney et al. 1985; Gasbarri et al. 1994; Kwon et al. 2008).

Here, we compared dopaminergic modulation of NMDAR-dependent early LTP in OR and RAD in acute hippocampal slices using D1R/D5R and D4R agonists. We blocked $GABA_A$Rs to avoid dopaminergic effects on inhibition and examined the AMPA component of glutamatergic transmission. Even though any NMDAR subtype constellation is capable of inducing NMDAR-dependent LTP in hippocampal RAD synapses (Berberich et al. 2005), dopaminergic modulation may lead to a preferential involvement of certain NMDAR subtypes. NMDARs containing NR2A have been proposed to interact with D1R/D5R (Lee et al. 2002; Varela et al. 2009), whereas NMDARs containing NR2B seem to interact with D2Rs (Liu

et al. 2006). Therefore, we explored NMDAR subtype dependency for both NMDA and AMPA components of excitatory postsynaptic currents (EPSCs) in constitutive NR2A knockout ($NR2A^{-/-}$) and forebrain-specific NR2B knockout mice ($NR2B^{\Delta Fb}$) in comparison with wild-type mice. We found that during LTP induction DA agonists activating D4Rs reduced the activity of NR2B-containing NMDARs in OR, causing input-specific modulation of LTP.

Materials and Methods

Experimental procedures were in accordance with the animal welfare guidelines of the Max Planck Society, the "Norwegian Animal Welfare Act" and the "European Union's Directive 86/609/EEC."

Immunohistochemistry

Z/EG mice (Novak et al. 2000) were crossbred with transgenic *DATCre* mice (Parlato et al. 2006) to generate Z/EG^{DATcre} reporter mice. Four-week-old Z/EG^{DATcre} mice were sacrificed with CO_2, perfused through heart with 4% paraformaldehyde/phosphate buffered saline (PFA/PBS) and brains were isolated and postfixed with 4% PFA/PBS at 4 °C overnight. Vibratome sections (50 μm thick) were stained for green fluorescent protein (GFP) with anti-GFP antibody (1:500, Invitrogen), biotinylated secondary anti-Rabbit antibody (Vector Laboratories), amplified by VECTASTAIN ABC kit (Vector Laboratories) and developed with 3,3′-diaminobenzidine (Sigma). Sections were mounted with Eukitt (Fluka). Images were taken on an Axioplan microscope (Zeiss) and processed with Adobe Creative Suite.

Extracellular Field Experiments

Wild-type (C57BL/6) mice (P27–P30) were killed with isoflurane. Transverse slices (400 μm) from the dorsal half of each hippocampus were cut with a vibroslicer in artificial cerebrospinal fluid (ACSF) containing (in mM): 123 NaCl, 4 KCl, 4 $MgCl_2$, 1.24 NaH_2PO_4, 4 $CaCl_2$, 26 $NaHCO_3$, and 12 D-glucose; 4 °C, pH 7.4 with 95% O_2/5% CO_2. Slices were placed in an interface chamber at 28–32 °C and perfused with ACSF containing 10 μM bicuculline methiodide (BMI) to block $GABA_A$ receptors. Orthodromic synaptic stimulation at 0.1 Hz was delivered alternately through 2 tungsten electrodes placed in the CA1 region, 1 in stratum radiatum (RAD), about 200 μm from pyramidal cell layer, and the other one in stratum oriens (OR), close to the alveus. Extracellular field excitatory postsynaptic potentials (fEPSPs) were monitored in the corresponding layers by 2 glass electrodes filled with ACSF and positioned 500–600 μm away from the stimulation electrodes. Synaptic efficacy and tetanization procedures were assessed as described earlier (Köhr et al. 2003). Six consecutive responses (1 min) were averaged and normalized to the mean value recorded 4–7 min before high-frequency stimulation (HFS: 100 Hz, 1 s). Data sets were pooled and presented as mean ± standard error of the mean (SEM). *n* indicates the number of slices. The subsequent number in brackets indicates the number of mice. Statistical evaluation was performed by using a paired or unpaired 2-tailed Student's *t*-test.

Whole-Cell Experiments

The brains were removed from deeply anesthetized (isoflurane) P27–P30 wild-type (C57BL/6), constitutive $NR2A^{-/-}$ (Sakimura et al. 1995) and forebrain-specific NR2B knockout mice ($NR2B^{\Delta Fb}$) (von Engelhardt et al. 2008). Hippocampal coronal slices (250 μm) were prepared, allowed to recover at 35 °C for 1 h, and thereafter maintained at room temperature (23–25 °C) in ACSF containing (in mM): 125 NaCl, 25 $NaHCO_3$, 2.5 KCl, 1.25 NaH_2PO_4, 2 $CaCl_2$, 1 $MgCl_2$, and 25 D-glucose; pH 7.4 with 95% O_2/5% CO_2 (320 mOsm). A slice was then transferred to a submerged recording chamber and continuously perfused with ACSF (1.5–2 mL/min) containing 10 μM BMI. Whole-cell recordings were performed at room temperature, using patch pipettes pulled from 0.5 mm walled borosilicate glass capillaries (Hilgenberg, Germany). Patch pipettes had resistances of 4–6.5 MΩ when filled with (in mM): 125 Cs-gluconate, 20 CsCl, 10 NaCl, 10 4-(2-hydroxyethyl)-1-piperazineethanesulfonic acid (HEPES), 0.2 ethyleneglycol-bis(2-aminoethylether)-*N,N,N′,N′*-tetra acetic acid (EGTA), 4 MgATP, 0.3 Na_3GTP, 2.5 QX-314Cl (pH 7.3, 270–320 mOsm). In some experiments, EGTA was increased to 10 mM. Liquid junction potentials were not corrected. Series and input resistances were monitored continuously by measuring peak and steady-state currents in response to hyperpolarizing pulses (−5 mV, 20 ms). The Schaffer collateral–commissural fibers were stimulated at 0.2 Hz with 2 glass electrodes filled with 1 M NaCl placed in RAD or in OR, 150 μm lateral from the recorded CA1 cell, and 150 and 50 μm away from the pyramidal cell layer, respectively. EPSCs were recorded at −70 mV. Six consecutive EPSCs were averaged and normalized to the responses obtained 5 min before washing in a DA agonist or before LTP induction and compared with responses obtained about 30 min later. For LTP recordings, the patch pipettes were filled with (in mM): 120 Cs-gluconate, 10 CsCl, 8 NaCl, 10 HEPES, 0.2 EGTA, 2 MgATP, 0.3 Na_3GTP, 10 phosphocreatine (pH 7.3, 270–320 mOsm), and the ACSF contained (in mM): 124 NaCl, 26 $NaHCO_3$, 2.5 KCl, 1.25 NaH_2PO_4, 4 $CaCl_2$, 4 $MgSO_4$, 10 D-glucose, and the NMDAR coagonist glycine (10 μM); pH 7.4 with 95% O_2/5% CO_2 (320 mOsm). LTP was induced by pairing postsynaptic depolarization (0 mV membrane potential for 3 min) with low-frequency synaptic stimulation (120 pulses, 0.67 Hz) of either the RAD or OR pathways (LFS pairing) (Chen et al. 1999), unpaired pathway served as a control. The average charge transfer per EPSC evoked during LFS pairing was determined by analyzing the 120 EPSCs individually. NMDAR-mediated EPSCs (NMDA EPSCs) were recorded in the presence of the AMPAR blocker NBQX (5 μM) at a membrane potential of +20 mV. NMDA EPSCs were elicited at 0.05 Hz, and if stable, they were normalized to 1 before applying the LFS pairing protocol at 0.67 Hz. The resulting NMDA EPSC inactivation was estimated either by averaging the peak amplitude or the charge transfer of 10 consecutive NMDA EPSCs during LFS pairing. To compare the decay times for NMDA EPSCs across different conditions, a weighted time constant ($\tau_{weighted}$) was calculated using the formula: $(I_{fast}/(I_{fast} + I_{slow})) \times \tau_{fast} + (I_{slow}/(I_{slow} + I_{fast})) \times \tau_{slow}$, where *I* is the amplitude of the fast or slow component. Data were pooled across animals of the same genotype and are presented as mean ± SEM. In addition to the number of cells (*n*), the number of slices (*x*) and mice (*y*) are presented in brackets (*x*, *y*). Statistical significance was evaluated by a 2-tailed Student's *t*-test (paired for washing in experiments and unpaired for all other experiments) or ANOVA with Fisher's post hoc analysis when comparing more than 2 pharmacological conditions or more than 2 genotypes at the same time.

Chemicals

NBQX and *R*-(+)-SCH23390 (both Biotrend), BMI and glycine (both Sigma), and SKF38393 and L-745,870 (both Tocris) were dissolved in water to stock solutions and further dissolved in the ACSF on the experimental day. PD168077 and *S*-(−)-sulpiride (both Biotrend), *R*(+)-6-bromo-APB (b-APB, Sigma), and clozapine (Tocris) were dissolved in dimethyl sulfoxide (DMSO) to a final DMSO concentration not exceeding 0.1%. The drugs were applied at least 15 min before whole-cell recordings or during washing in. G-proteins were blocked by adding GDPßS (1 mM, Sigma) to the aliquots of the electrode solutions, while holding pH and osmolarity constant. GDPßS was allowed to diffuse into the cell for at least 25 min prior to baseline recordings.

Results

Distribution of Dopamine Active Transporter within Hippocampal Area CA1

Neuronal tracer techniques combined with immunocytochemistry have revealed a differential dopaminergic innervation of the hippocampal formation in rats (Gasbarri et al. 1994; Gasbarri et al. 1997). Therefore, the rat dopamine active transporter (DAT), which is enriched in dopaminergic terminals (Cragg and Rice 2004) could also be differentially distributed. To visualize DAT-enriched fibers in mice, we employed a reporter mouse (Z/EG^{DATcre}) which expresses GFP in cells expressing DAT. Thus, via projections of dopaminergic neurons

residing in the pars compacta of substantia nigra, the dorsal striatum was intensively stained in sections from 6 Z/EG^{DATcre} mice (Fig. 1*A*). Staining was more pronounced in stratum oriens (OR) than in stratum radiatum (RAD) within the dorsal hippocampal CA1 region. Higher resolution images showed DAT-stained fibers passing along the alveus in sagittal sections and ending radially in coronal sections in OR (Fig. 1*A*; see also dopaminergic innervation in OR obtained by immunofluorescence in Kwon et al. 2008). Although we could not observe DAT-stained fibers in RAD, we cannot rule out that dopaminergic input is also conveyed via fibers in RAD.

Low-Frequency Stimulation

In order to unmask whether the skewed distribution of dopaminergic fibers modulated the glutamatergic transmission in the mouse hippocampal slice preparation, we evoked EPSCs by LFS (0.2 Hz) of the RAD and the OR pathways. We blocked the $GABA_A$-mediated inhibition by bicuculline (BMI, 10 μM) to avoid effects of dopamine agonists on inhibitory transmission. Forty minutes of washing in the D1R/D5R agonist SKF38393 (50 μM) failed to affect EPSCs elicited in the 2 pathways (OR: 0.93 ± 0.16, n = 6, P = 0.64; RAD: 0.96 ± 0.09, n = 6 (6, 6), P = 0.67) (Fig. 1*B*). The present results extend earlier reports showing that the AMPA component of EPSCs in RAD was not modulated by DA agonists during single-pulse stimulation (Otmakhova and Lisman 1996; Mockett et al. 2004).

High-Frequency Stimulation

In wild-type mice, HFS (100 Hz, 1 s) of either the RAD or the OR pathway in the presence of BMI (10 μM) produced a persisting homosynaptic potentiation of extracellular fEPSPs 40–45 min after the tetanization, characteristic of early LTP of

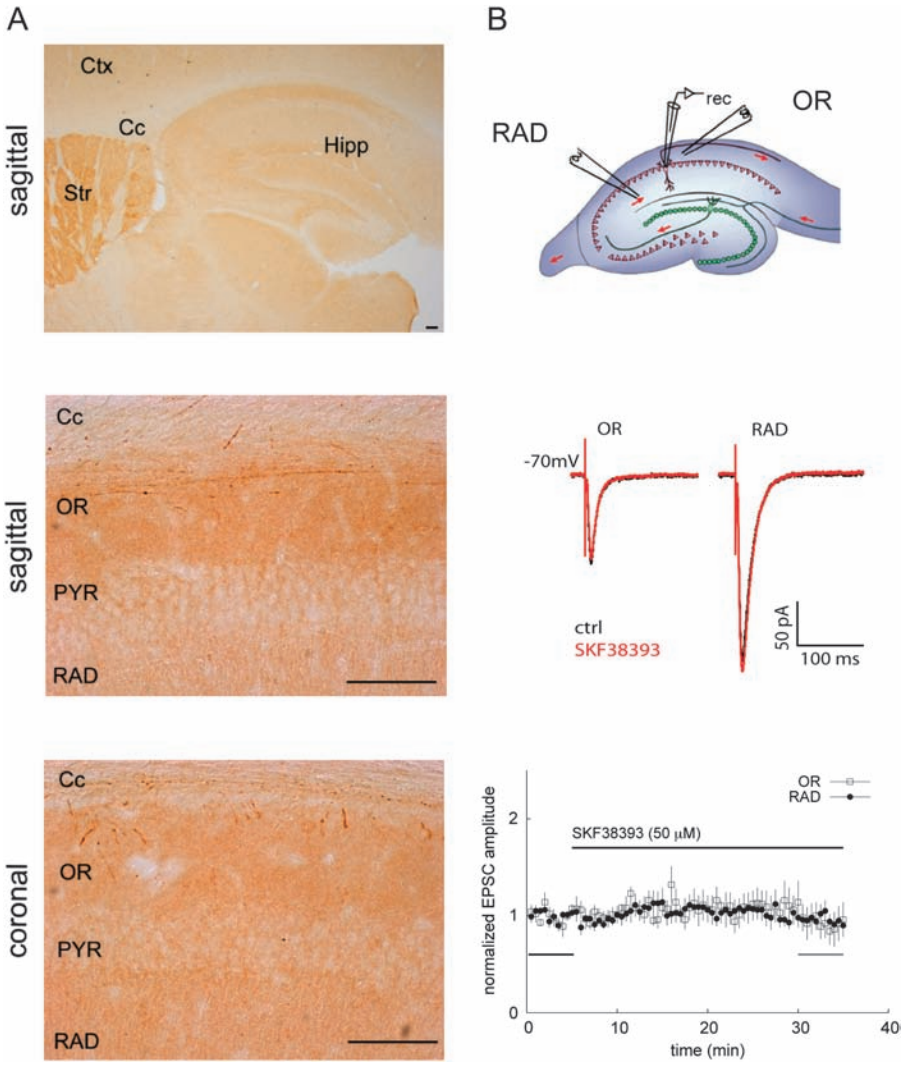

Figure 1. DAT-positive fibers and excitatory postsynaptic transmission in CA3-to-CA1 synapses in the presence of SKF38393. (*A*) GFP immunostaining of DAT-positive fibers. Upper panel shows intensive staining of striatum (Str) and within hippocampus (Hipp) in a sagittal section (50 μm) from the *Z/EG^{DATcre}* reporter mouse. Abbreviations: Ctx, neocortex; Cc, corpus callosum; Scale bar, 100 μm. Lower panels show intensive staining of dopaminergic projections to stratum oriens (OR) when compared with stratum radiatum (RAD) of hippocampal CA1, both in a sagittal section where stained fibers project along the alveus and in a coronal section where stained fibers end radially. PYR marks the pyramidal cell layer. Scale bar, 100 μm. (*B*) Upper panel shows a schematic drawing of a hippocampal section where 1 recording and 2 stimulation electrodes were placed in OR and RAD. Middle panel shows superimposed means of 30 consecutive EPSCs evoked by stimulation in OR or RAD at −70 mV membrane potential in CA1 neurons prior to (black traces) and about 30 min after washing in 50 μM SKF38393 (red traces). EPSCs were averaged from time periods indicated by bars in the lower panel, which shows normalized EPSC amplitudes from the OR and the RAD pathways during bath perfusion of 50 μM SKF38393, relative to baseline, that is, absence of drug. Data are shown as mean ± SEM.

synaptic transmission. The magnitude of LTP was comparable in the 2 CA1 pathways (OR: 1.26 ± 0.04, $n = 16$ (9); RAD: 1.39 ± 0.06, $n = 21$ (9), $P = 0.09$) (Fig. 2*A,B*), whereas the untetanized control pathway remained unchanged. This indicates that in our slice preparation branches from CA3 axons, targeting both OR and RAD, hardly contribute to evoked responses. In presence of 50 μM SKF38393, the tetanization elicited a less pronounced posttetanic potentiation/short-term potentiation phase ($P < 0.05$ for the initial 8 min in OR and the initial 3 min in RAD after tetanization) (Fig. 2*A,B*). In contrast, 40–45 min after the tetanization LTP was strongly reduced in OR (1.07 ± 0.05, $n = 14$ (8), $P = 0.008$) but only marginally in RAD (1.21 ± 0.06, $n = 15$ (9), $P = 0.04$) (Fig. 2*A,B*). These results contrast with very recent observations, which showed enhanced field LTP both in OR and in RAD when using 20 μM SKF38393 in rat hippocampal slices with intact $GABA_A$ receptor mediated inhibition (Stramiello and Wagner 2008, 2010). Therefore, our results in presence of BMI unmask a pathway-specific dopaminergic modulation on glutamatergic transmission.

LFS Pairing at Membrane Potentials of 0 and +20 mV

Next, we used whole-cell recordings in the presence of BMI (10 μM) to examine in the 2 dendritic CA1 subfields the effect of SKF38393 on AMPAR- as well as NMDAR-mediated currents. Following a period with stable synaptic responses (EPSCs) elicited at 0.2 Hz, LFS at 0.67 Hz was paired with postsynaptic depolarization of 0 mV membrane potential for 3 min (Chen et al. 1999). In presence of SKF38393 (50 μM), the amount of LTP obtained 30 min after LFS pairing was similar to LTP

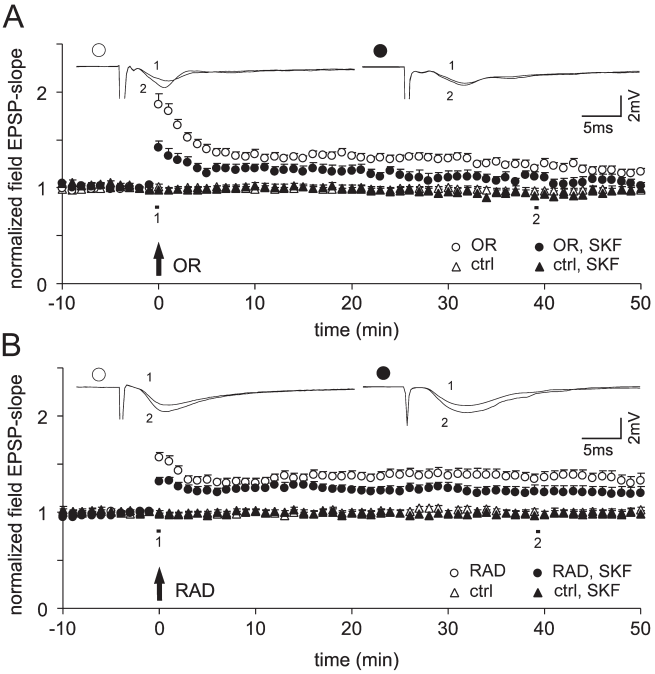

Figure 2. Extracellular LTP in presence of bicuculline and SKF38393 in stratum oriens and stratum radiatum. (*A*) Normalized and pooled extracellular slopes from fEPSPs evoked at CA3-to-CA1 synapses in stratum oriens (OR) in acute slices without (open symbols, $n = 16$) or with 50 μM SKF38393 present (filled symbols, $n = 14$). The tetanized pathways are shown as circles, the untetanized control pathways are shown as triangles. The insets show the mean of 6 consecutive synaptic responses before 1) and 40 min after 2) tetanization in the 2 conditions. (*B*) As in *A*, but results are from RAD ($n = 21$ and $n = 15$, respectively). Arrow, time point of tetanic (high-frequency) stimulation. Data are shown as mean ± SEM.

obtained in the control solution in the RAD pathway (control solution: 2.52 ± 0.17, $n = 6$ (4, 3); with SKF: 2.35 ± 0.38, $n = 8$ (7, 6); $P = 0.68$), However, in the OR pathway, LTP was significantly reduced (control solution: 1.99 ± 0.16, $n = 9$ (7, 7); with SKF: 1.34 ± 0.14, $n = 7$ (4, 4) $P < 0.05$) (Fig. 3*A,B*). Since $GABA_A$ receptors were blocked, the results indicate a direct modulatory effect of SKF38393 on excitatory synaptic transmission in OR. In addition, analysis of the EPSC charge transfer during the LFS pairing paradigm at 0 mV revealed a selective statistically significant decreased charge transfer in presence of SKF38393 in the OR pathway (OR, control solution: –2.73 ± 0.39 pC, $n = 9$ (7, 7); OR with SKF: –0.89 ± 0.16 pC, $n = 7$ (4, 4), $P < 0.01$; RAD, control solution: –4.44 ± 0.5 pC, $n = 6$ (4, 3); RAD with SKF: –3.62 ± 1.15 pC, $n = 8$ (7, 6), $P = 0.53$) (Fig. 3*C*). Thus, the reduced LTP in OR in the presence of SKF38393 could be due to a reduced Ca^{2+} influx through NMDARs during the LFS pairing paradigm.

To further elucidate whether NMDARs are modulated by D1R/D5R agonists during LTP induction, we recorded at +20 mV membrane potential synaptic NMDAR-mediated currents (NMDA EPSCs) while blocking AMPARs (5 μM NBQX). Following baseline responses elicited at 0.05 Hz, we applied the LFS pairing protocol (Fig. 4). During the LFS pairing protocol, peak amplitudes and charge transfers of NMDA EPSCs gradually decreased in both OR and RAD (Fig. 4*B,C*). These decreases in NMDAR-mediated responses were significantly and selectively accentuated in the presence of SKF38393 in the OR pathway. On average, the NMDAR-mediated charge transfer, which is correlated to whether LTP develops (Berberich et al. 2007), was reduced by ~35% in OR (OR relative to baseline with control solution: 0.73 ± 0.03, $n = 22$ (18, 14); OR with SKF: 0.46 ± 0.04, $n = 7$ (5, 5), $P < 0.0001$), whereas no effect was observed at RAD synapses (RAD relative to baseline with control solution: 0.59 ± 0.03, $n = 6$ (6, 6); RAD with SKF: 0.63 ± 0.06, $n = 7$ (2, 2), $P = 0.44$) (Fig. 4*D*). Therefore, the D1R/D5R agonist SKF38393 seems to interfere with LTP induction in the OR pathway through an augmented inactivation of NMDA EPSCs.

We also found a similar pathway-specific dopaminergic modulation of the NMDA EPSC charge transfer in presence of *R*(+)-6-bromo-APB (b-APB, 50 μM), another D1R/D5R agonist (Otmakhova and Lisman 1996; Navakkode et al. 2007) (OR, control solution: 0.73 ± 0.03, $n = 22$ (18, 14); OR with b-APB: 0.56 ± 0.04, $n = 7$ (4, 3), $P < 0.01$; RAD, control solution: 0.59 ± 0.05, $n = 6$ (6, 6); RAD with b-APB: 0.64 ± 0.06, $n = 9$ (6, 3), $P = 0.43$) (Fig. 4*E*).

The Involvement of NR2A and NR2B Subunits

D1Rs have been reported to interact directly with NR1 and NR2A subunits in heterologous cells and cultured hippocampal neurons (Lee et al. 2002), whereas D2Rs are known to interact directly with NR2B subunits in striatal neurons (Liu et al. 2006). Based on our observed pathway-specific dopaminergic modulation of NMDAR activity during the LFS pairing paradigm and the subsequent reduction in the amount of LTP, we examined NR1/NR2B receptors in *NR2A*$^{-/-}$ mice and NR1/NR2A in *NR2B*$^{\Delta Fb}$ mice to determine if either NR2A- or NR2B-containing NMDARs might be a preferential target for DA agonist modulation. In the hippocampus of adult (>P60) *NR2B*$^{\Delta Fb}$ mice, NR2B protein expression is absent in most forebrain neurons, and in these neurons, the decay time of NMDA EPSCs

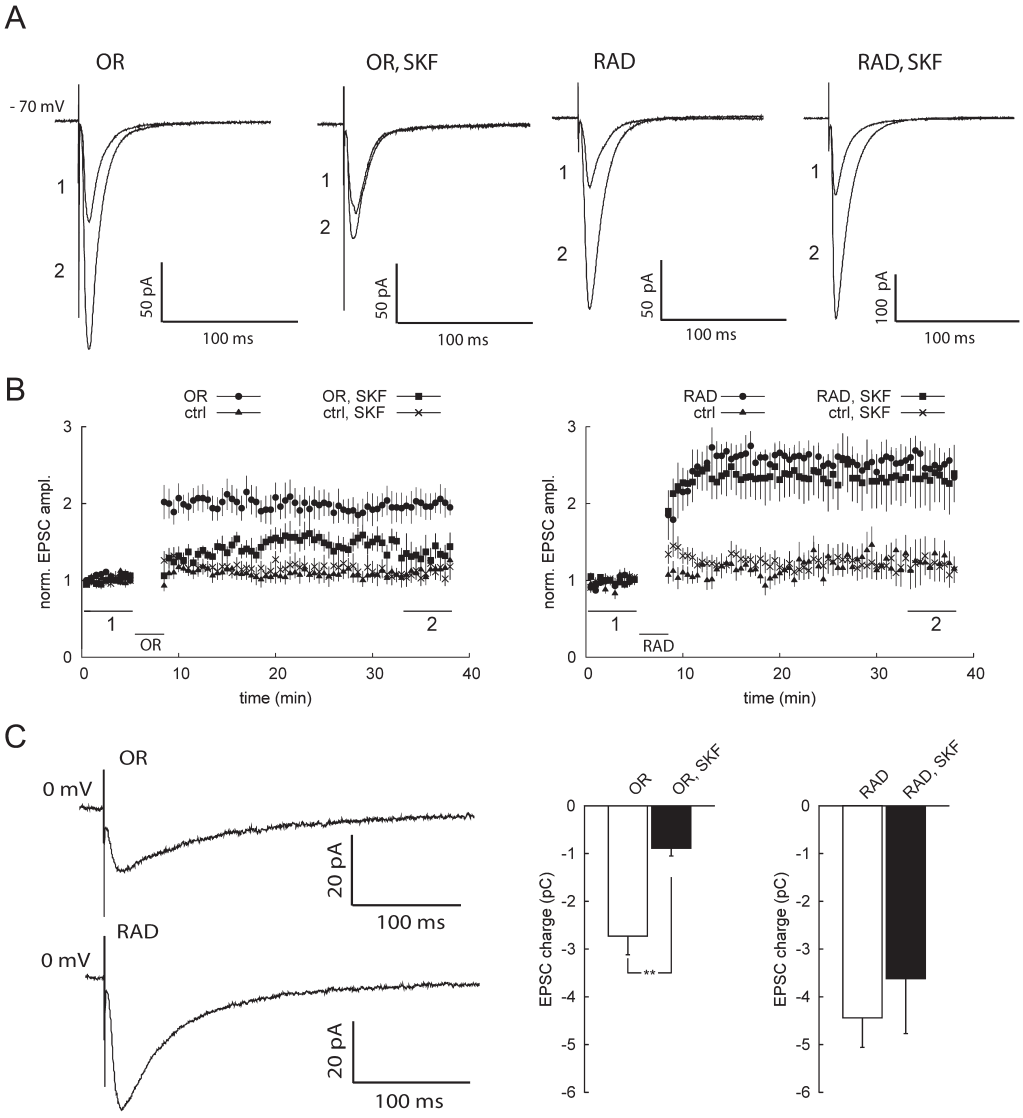

Figure 3. Whole-cell LTP and charge transfer during LTP induction in the presence of SKF38393. (*A*) Superimposed means of 60 EPSCs recorded at −70 mV membrane potential prior to 1) and after 2) LFS pairing at 0 mV membrane potential in the absence or presence of 50 μM SKF38393 (left, OR; right, RAD). The superimposed means are taken from time periods 1 and 2 marked with horizontal bars in *B*. (*B*) Normalized and pooled ($n = 6$) EPSC amplitudes evoked in OR and RAD without or with 50 μM SKF38393 present. The time period of LFS pairing is indicated by the horizontal bar (OR, left; RAD, right). The respective unpaired control pathways are also shown. Note the selective reduction of LTP in OR. (*C*) Mean of 120 EPSCs evoked during LFS pairing at 0.67 Hz in the test pathway OR or RAD both in the absence of SKF38393. The bars show the averaged EPSC charge transfer during LFS pairing in OR (left) and RAD (right) in the absence (open) and presence (filled) of 50 μM SKF38393. Note the selective reduction of charge transfer in OR. ** indicates $P < 0.01$. Data are shown as mean ± SEM.

is significantly faster than in wild type (von Engelhardt et al. 2008; Rauner and Köhr 2011). In slices from *NR2B*$^{\Delta Fb}$ mice at P27–P29, we restricted our analysis to cells that had NMDA EPSCs with fast decay.

Analogous to wild-type mice, the NMDA EPSC charge transfer was examined in the mutants at +20 mV membrane potential during the LFS pairing paradigm in absence and presence of SKF38393 (Fig. 5). In slices from *NR2A*$^{-/-}$ mice (Fig. 5*A*), as observed in wild type (Fig. 4*C*), SKF38393 significantly reduced the NMDA EPSC charge transfer in OR but not in RAD (OR, control solution: 0.73 ± 0.06, $n = 7$ (4, 3); OR with SKF: 0.48 ± 0.04, $n = 8$ (6, 4), $P < 0.05$; RAD; control solution: 0.68 ± 0.04, $n = 7$ (6, 2); RAD with SKF: 0.67 ± 0.07, $n = 7$ (6, 3), $P = 0.96$). In slices from *NR2B*$^{\Delta Fb}$ mice, however, SKF38393 failed to affect the inactivation of NMDA EPSCs in both layers (OR, control solution: 0.51 ± 0.11, $n = 4$ (3, 2); OR with SKF: 0.4 ± 0.05, $n = 4$ (4, 3), $P = 0.51$; RAD, control solution: 0.66 ± 0.04, $n = 5$ (3, 2); RAD with SKF: 0.56 ± 0.05, $n = 6$ (3, 2), $P = 0.21$) (Fig. 5*B*). These results suggest that the applied DA agonist selectively modulated NMDA EPSC charge transfer in OR via NMDARs containing NR2B subunits (Fig. 5*C*).

LFS Pairing at 0 mV in NR2B$^{\Delta Fb}$ and *NR2A*$^{-/-}$ Mice

In accordance with von Engelhardt et al. (2008), LTP was significantly reduced in the RAD pathway of *NR2B*$^{\Delta Fb}$ mice following the LFS pairing paradigm (RAD: 1.54 ± 0.1, $n = 9$ (5, 5), $P < 0.01$) (Fig. 6*A*,*B*). We also found a similar reduction of LTP in the OR pathway (OR: 1.33 ± 0.15, $n = 8$ (6, 4), $P < 0.05$) (Fig. 6*A*,*B*). As expected from the analysis of the charge transfer mediated by NMDA EPSCs, which was not affected by SKF38393 (Fig. 5*B*), the presence of SKF38393 failed to

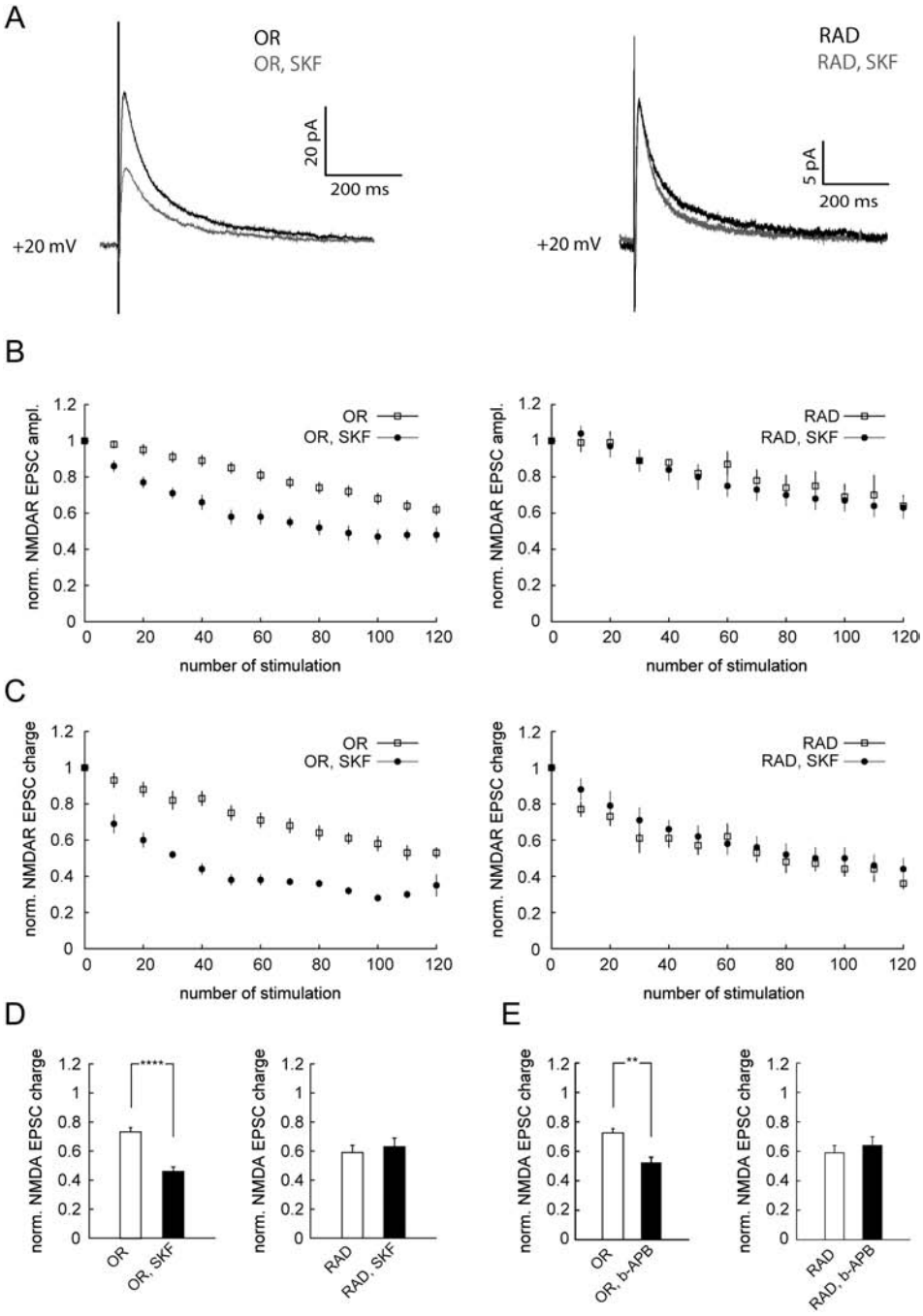

Figure 4. NMDAR-mediated EPSC peak currents and charge transfer during LFS pairing in the presence of SKF38393. One hundred and twenty LFS pairings were performed at +20 mV membrane potential during AMPAR blockade (NBQX, 5 μM). (*A*) Superimposed mean traces of NMDA EPSCs ($n = 120$) recorded in different slices in the absence (black) or presence (gray) of 50 μM SKF38393 (OR, left; RAD, right). (*B*) Pooled ($n = 10$) NMDA EPSC amplitudes, recorded during LFS pairing at 0.67 Hz in control solution (open symbols) and in the presence of 50 μM SKF38393 (filled symbols), were normalized to NMDA EPSCs evoked before at 0.05 Hz (left, OR; right, RAD). (*C*) As in *B*, but the graphs show the corresponding NMDAR-mediated charge transfer. (*D*) Averaged NMDA EPSC charge transfer during LFS pairing at +20 mV membrane potential in OR (left) and RAD (right) in the absence and presence of 50 μM SKF38393. (*E*) As in *D*, but in the presence of 50 μM b-APB. Note the selective reduction of charge transfer in OR in the presence of both drugs. ** and **** indicate $P < 0.01$ and $P < 0.0001$, respectively. Data are shown as mean ± SEM.

modulate the magnitude of LTP both in RAD and in OR (RAD: 1.49 ± 0.15, $n = 9$ (6, 5), $P = 0.82$; OR: 1.38 ± 0.14, $n = 8$ (4, 3), $P = 0.83$). Analysis of the charge transfer during LFS pairing at 0 mV membrane potential substantiated this finding (Fig. 6*C*) because SKF38393 failed to alter the EPSC charge in both pathways (RAD, control solution: −5.36 ± 1.71 pC, $n = 9$ (5, 5); RAD with SKF: −4.91 ± 1.7 pC, $n = 9$ (6, 5), $P = 0.86$; OR, control solution: −1.28 ± 0.27 pC, $n = 8$ (6, 4), OR with SKF: −0.83 ± 0.09 pC, $n = 8$ (4, 3), $P = 0.20$). It is therefore unlikely that NR1/NR2A receptors are responsible for the SKF38393-mediated reduction of LTP in OR in wild-type mice. Therefore, the dopaminergic modulation of LTP in OR in wild-type mice might possibly be ascribed to NR2B-containing NMDARs.

To support this conclusion, we employed *NR2A*$^{-/-}$ mice (Sakimura et al. 1995) and induced LTP in the 2 pathways by LFS pairing (Fig. 7). LTP in OR was comparable to that obtained

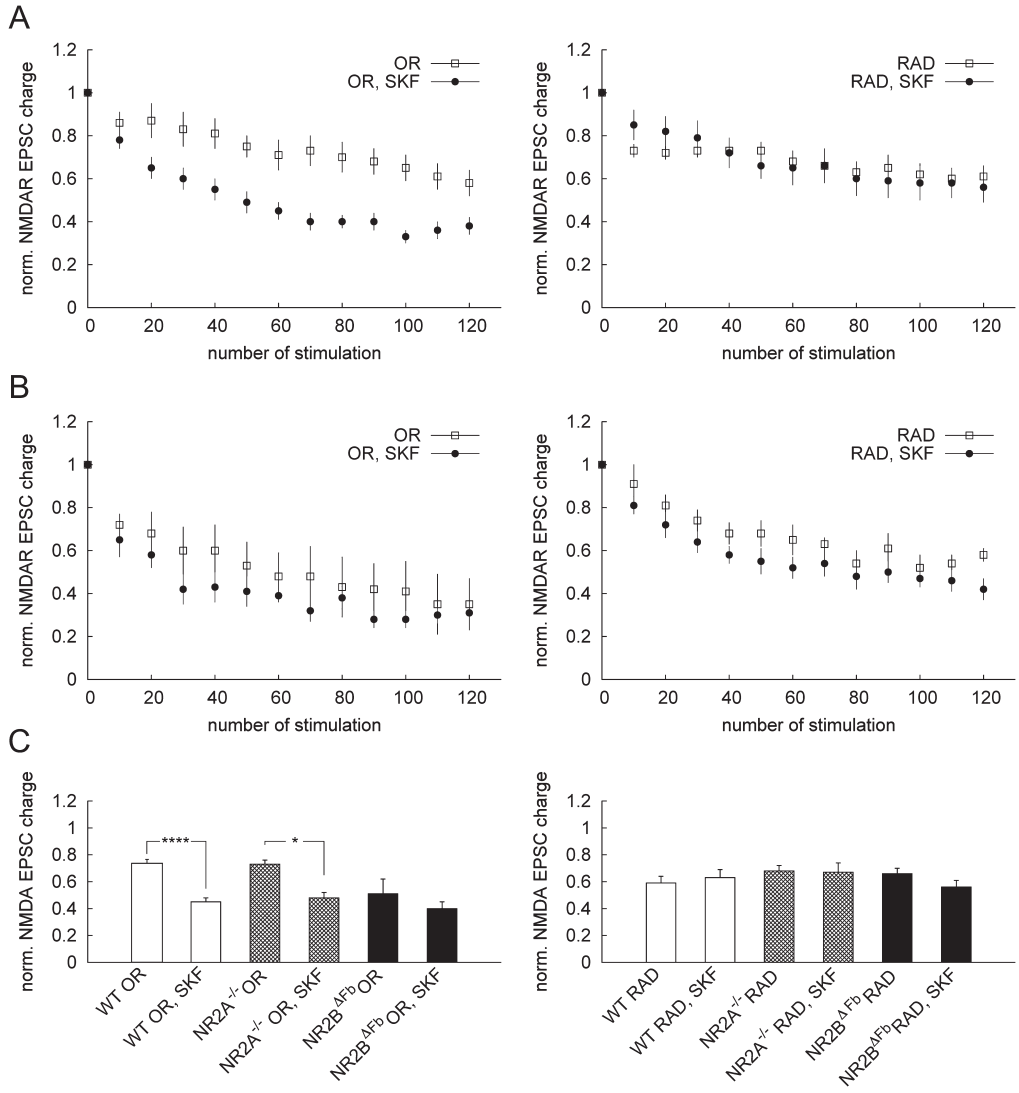

Figure 5. NMDAR-mediated EPSC charge transfer during LFS pairing in the presence of SKF38393 in 2 NR2 mutant mice. One hundred and twenty LFS pairings were performed at +20 mV membrane potential during AMPAR blockade (NBQX, 5 μM). (*A*) Normalized and pooled (n = 10) NMDA EPSC charge transfer in *NR2A*$^{-/-}$ mice in the absence or presence of 50 μM SKF38393. (*B*) As in *A*, but in *NR2B*$^{\Delta Fb}$ mice. (*C*) Summary graph regarding NMDA EPSC charge transfer in wild-type *NR2A*$^{-/-}$ and *NR2B*$^{\Delta Fb}$ mice and its modulation by 50 μM SKF38393 in OR (left graph) and RAD (right graph). Note a selective SKF38393-mediated effect in OR through NMDARs containing NR2B subunits. * and **** indicate $P < 0.05$ and $P < 0.0001$, respectively. Data are shown as mean ± SEM.

in wild-type mice in OR (1.94 ± 0.21, n = 8 (5, 4), P < 0.83), whereas LTP in RAD was significantly reduced (1.78 ± 0.09, n = 8 (6, 4), P < 0.01). In the presence of SKF38393, LTP in OR was reduced (1.38 ± 0.14, n = 10 (5, 3), P < 0.05), whereas SKF failed to modulate LTP in RAD (1.62 ± 0.09, n = 10 (7, 5), P = 0.23). Analysis of the charge transfer at 0 mV during the LFS pairing supported this finding (Fig. 7*C*), revealing a significant charge reduction in OR but not in RAD (OR, control solution: –4.85 ± 0.29 pC, n = 8 (5, 4); OR with SKF: –0.85 ± 0.13 pC, n = 10 (5, 3), P < 0.0001; RAD; control solution: –4.01 ± 0.62 pC, n = 8 (6, 4); RAD with SKF: –3.44 ± 0.43 pC, n = 10 (7, 5), P = 0.48). These results indicate that the dopaminergic modulation of LTP induction in OR is closely linked to NR2B-containing NMDARs.

Dopaminergic Modulation of NMDAR Activity in Stratum Oriens is Ca^{2+} dependent and G-protein independent

Changes in intracellular Ca^{2+} through NMDARs are necessary for long-term changes in synaptic AMPAR function (reviewed in Malenka and Bear 2004). Intracellular Ca^{2+} is also known to rise following the activation of DA receptors (Hasbi et al. 2010) and may contribute to the Ca^{2+}-dependent inactivation of NMDARs (Zhang et al. 1998; Krupp et al. 1999; Kotecha et al. 2002). To test Ca^{2+} dependencies regarding the dopaminergic modulation of NMDA EPSCs in OR, we used 10 mM EGTA in the patch pipette (Fig. 8*A*). In the absence of SKF, the charge transfer of NMDA EPSCs evoked at +20 mV in OR was reduced to a similar degree in 0.2 and 10 mM EGTA (0.2 mM, 0.73 ± 0.03, n = 22 (18, 14), Fig. 4*C*; 10 mM, 0.69 ± 0.07, n = 7 (6, 4), P = 0.65; Fig. 8*A*). In contrast, the SKF38393-augmented inactivation of NMDA EPSCs in OR was no longer observed in the presence of 10 mM EGTA (with SKF: 0.61 ± 0.1, n = 7 (6, 4), P = 0.51; Fig. 8*A*). This indicates a Ca^{2+} dependency of the observed dopaminergic NMDA EPSCs modulation in OR.

Different intracellular signaling systems have been linked to DA receptors. Receptor coupling to Gs- and Gi-proteins regulate the adenylate cyclase catalysis of cAMP formation, whereas coupling to Gq-proteins works through the PLC/IP3

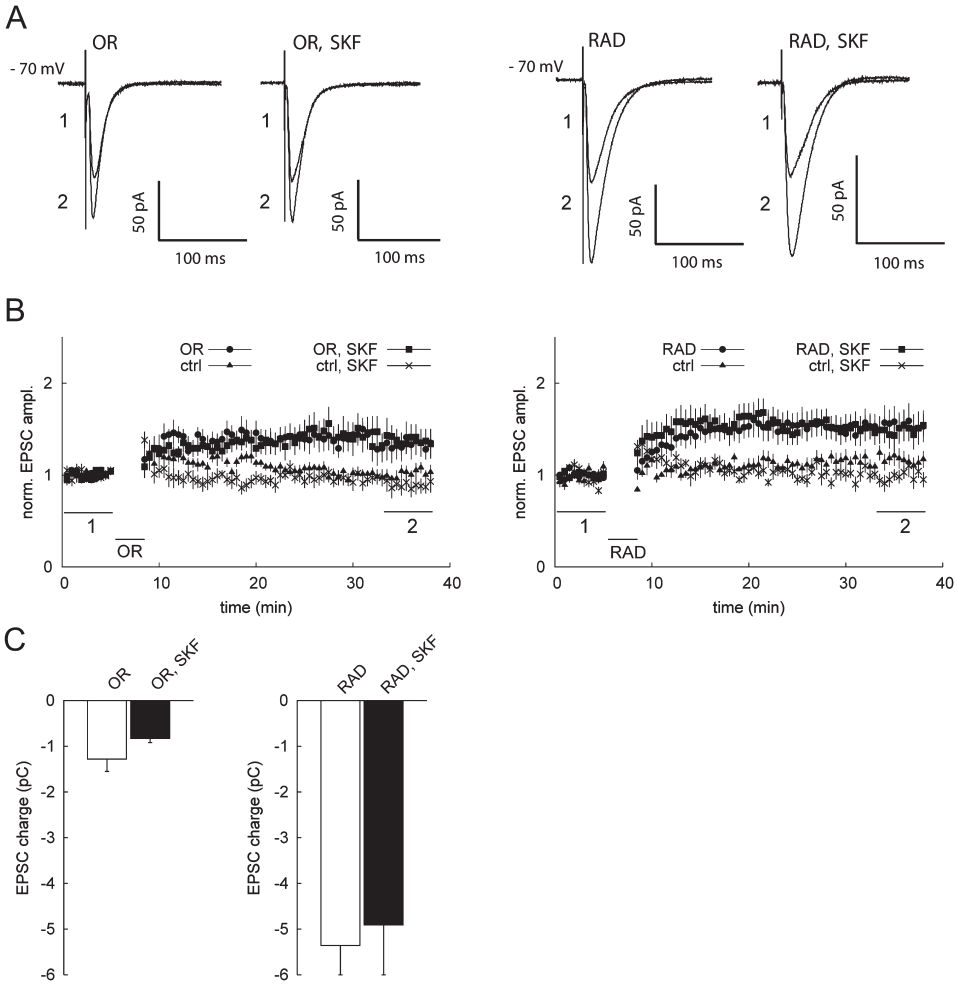

Figure 6. Whole-cell LTP and charge transfer during LTP induction in the presence of SKF38393 in slices from *NR2B*$^{\Delta Fb}$ mice. (*A*) Superimposed means of 60 EPSCs recorded at −70 mV membrane potential prior to 1) and after 2) LFS pairing at 0 mV membrane potential in the absence or presence of 50 μM SKF38393 (left, OR; right, RAD). The superimposed means are taken from time periods 1 and 2 marked with horizontal bars in *B*. (*B*) Normalized and pooled ($n = 6$) EPSC amplitudes evoked in OR and RAD without or with 50 μM SKF38393 present. The time period of LFS pairing is indicated by the horizontal bar (OR, left; RAD, right). The respective unpaired control pathways are also shown. (*C*) Averaged EPSC charge transfer during LFS pairing in OR (left) and RAD (right) in the absence (open) and presence (filled) of 50 μM SKF38393. Note that neither LTP nor charge transfer is modulated by SKF38393 in OR or RAD. Data are shown as mean ± SEM.

pathway (Hasbi et al. 2010). We inhibited G-proteins by allowing the stable GDP analog guanosine 5′-*O*-2-thiodiphosphate (GDPßS, 1 mM) to diffuse into the CA1 neuron via the patch pipette 25 min prior to baseline recordings. The presence of GDPßS did not affect the reduction of NMDA EPSC charge transfer in OR, neither in absence nor in presence of SKF38393 (control solution, $P = 0.29$; with SKF, $P = 0.14$). Consequently, the SKF effect remained significant in OR (control solution, 0.68 ± 0.04, $n = 9$ (2, 1), with SKF, 0.50 ± 0.03, $n = 9$ (4, 4), $P < 0.001$; Fig. 8*B* and for absence of GDPßS, see Fig. 4*C*). Thus, DA receptor–mediated activation of G-proteins does not appear to contribute to the modulation of NMDA EPSCs in OR.

Effects of Dopamine Receptor Agonists and Antagonists in Stratum Oriens

To elucidate whether the modulation of NMDA EPSCs in OR by SKF38393 and b-APB during the LFS pairing protocol at +20 mV (see Fig. 4) were mediated via D1-like receptors, we examined the NMDA EPSC charge transfer in the presence of both the SKF38393 (50 μM) and the D1R/D5R antagonist SCH23390 (1 or 10 μM). Surprisingly, the SKF38393-induced augmentation of NMDA EPSC inactivation in OR was not antagonized by SCH23390 (1 μM, 0.38 ± 0.05, $n = 4$ (1, 1), $P < 0.01$; 10 μM, 0.45 ± 0.04, $n = 11$ (5, 5), $P < 0.01$) (Fig. 8*C*). The D2R antagonist sulpiride behaved in a similar way (15 μM, 0.33 ± 0.04, $n = 4$ (2, 1), $P < 0.01$) (Fig. 8*C*). The reported existence of D1/D2 heterooligomers (Hasbi et al. 2010) led us coperfuse SCH23390 (1 μM) and sulpiride (10 μM), which has a 100-fold higher affinity to D2Rs and D3Rs than to D4Rs (Seeman and Van Tol 1994). Although the SKF38393-induced reduction in NMDA EPSC charge transfer was synergistically diminished ($P < 0.05$), SCH23390 and sulpiride together failed to fully antagonize the SKF38393-mediated modulation (0.56 ± 0.07, $n = 5$ (2, 1), $P < 0.05$) (Fig. 8*C*). These experiments indicated that D1R/D5Rs and D2R/D3Rs with high affinity to sulpiride are not involved in the modulation of NMDA EPSCs in stratum oriens.

Next, we considered the contribution of D4Rs, which negatively regulate NMDAR transmission and LTP in rat hippocampal slices (Kotecha et al. 2002; Stramiello and Wagner

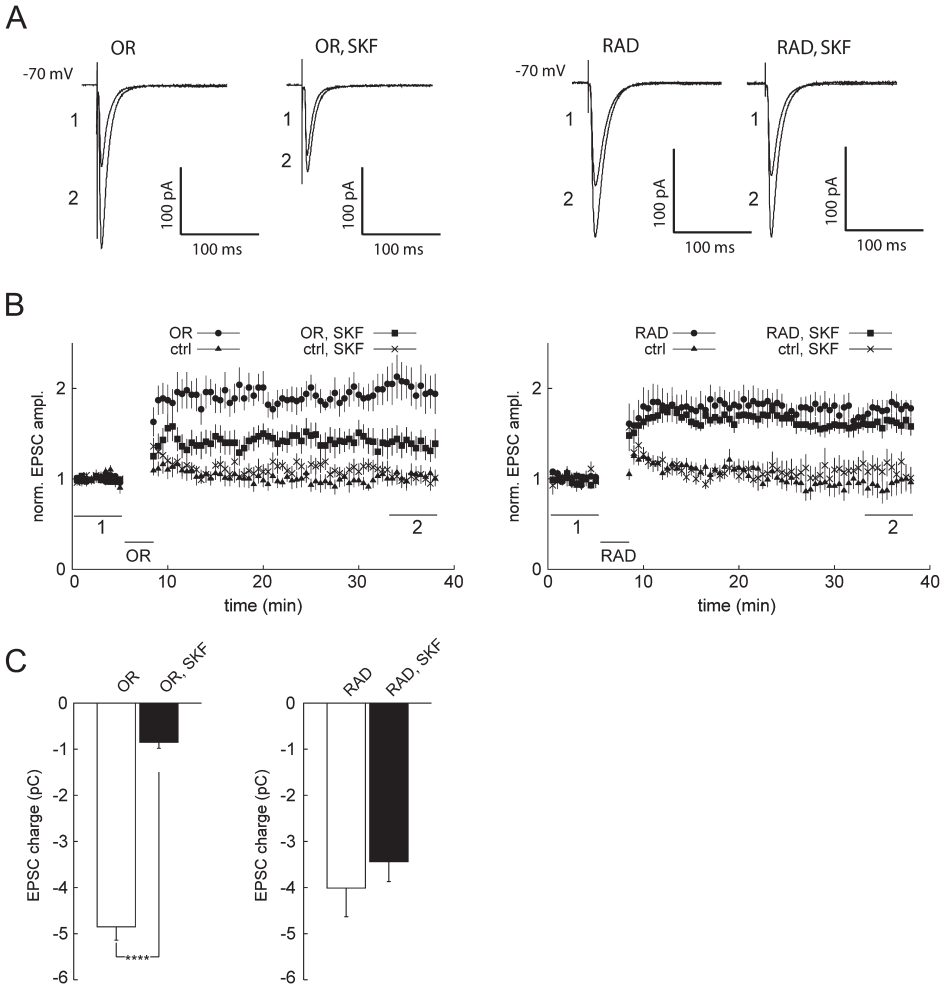

Figure 7. Whole-cell LTP and charge transfer during LTP induction in the presence of SKF38393 in slices from *NR2A*$^{-/-}$ mice. (*A*) Superimposed means of 60 EPSCs recorded at −70 mV membrane potential prior to 1) and after 2) LFS pairing at 0 mV membrane potential in the absence or presence of 50 μM SKF38393 (left, OR; right, RAD). The superimposed means are taken from time periods 1 and 2 marked with horizontal bars in *B*. (*B*) Normalized and pooled ($n = 6$) EPSC amplitudes evoked in OR and RAD without or with 50 μM SKF38393 present. The time period of LFS pairing is indicated by the horizontal bar (OR, left; RAD, right). The respective unpaired control pathways are also shown. (*C*) Averaged EPSC charge transfer during LFS pairing in OR (left) and RAD (right) in the absence (open) and presence (filled) of 50 μM SKF38393. Note that LTP and charge transfer are modulated by SKF38393 in OR but not in RAD. **** indicates $P < 0.0001$. Data are shown as mean ± SEM.

2008). First, we tested clozapine (20 μM), an atypical neuroleptic with a relatively high affinity for D4Rs compared with other DA receptors. This compound blocked the SKF-induced decrease in charge transfer (0.66 ± 0.09, $n = 6$ (5, 3), $P = 0.32$) (Fig. 8*C*). Because clozapine also has affinity to alpha-adrenergic and serotonergic receptors (reviewed in Meltzer 1995; Svensson 2003), we subsequently applied the potent and selective D4R antagonist L-745,870 (100 nM) which also fully blocked the SKF-induced decrease in charge transfer (0.67 ± 0.07, $n = 5$ (2, 2), $P = 0.92$; Fig. 8*C*). These experiments indicated that SKF38393 at 50 μM is nonselective, since SKF38393 not only binds to D1Rs but also to D4Rs, which in turn modulated NMDA EPSCs in OR.

To explore whether a selective activation of D4Rs was sufficient to reduce the NMDA EPSC charge transfer, we applied the LFS pairing protocol at +20 mV in the presence of the selective D4R agonist PD168077 (100 nM). PD168077 augmented the reduction in the OR but not in the RAD pathway (OR, control solution: 0.73 ± 0.03, $n = 22$ (18, 14); OR with PD168077: 0.53 ± 0.04, $n = 8$ (5, 3), $P < 0.01$; RAD, control solution: 0.72 ± 0.08, $n = 4$ (2, 2); RAD with PD168077: 0.82 ± 0.05, $n = 7$ (2, 2), $P = 0.25$) (Fig. 8*D*). This input-specific effect by PD168077 was completely blocked by the selective D4R antagonist L-745,870 (50 nM; 0.68 ± 0.05, $n = 6$ (2, 2), $P = 0.81$) (Fig. 8*D*). Thus, the dopaminergic modulation of NMDA EPSCs in OR appears to be exclusively mediated via D4Rs.

In a last set of experiments, we tested the possibility that the D4R-mediated modulation of NMDAR function affects LTP in wild-type mice. First, we evoked stable EPSCs at –70 mV at 0.2 Hz before washing in PD168077 at 100 nM, which did not affect the peak amplitude of EPSCs in wild-type mice (OR: 0.95 ± 0.06, $n = 11$ (11, 4), $P = 0.59$; RAD: 1.09 ± 0.1, $n = 11$ (11, 4), $P = 0.42$) (Fig. 8*E*). In separate experiments and in continuous presence of 100 nM PD168077, we applied the LFS pairing protocol in OR, which significantly reduced LTP compared with control experiments lacking the D4R antagonist (control solution: 1.99 ± 0.16, $n = 9$ (7, 7); with PD168077: 1.23 ± 0.08, $n = 9$ (7, 5), $P < 0.01$). Thus, PD168077 reflects all functional aspects that we had observed with SKF38393 at 50 μM (Figs 1*B*, 3*B*, and 4*D*), indicating that the suppression of LTP in OR by PD168077 or SKF38393 was caused through modulation of NMDAR function via D4Rs.

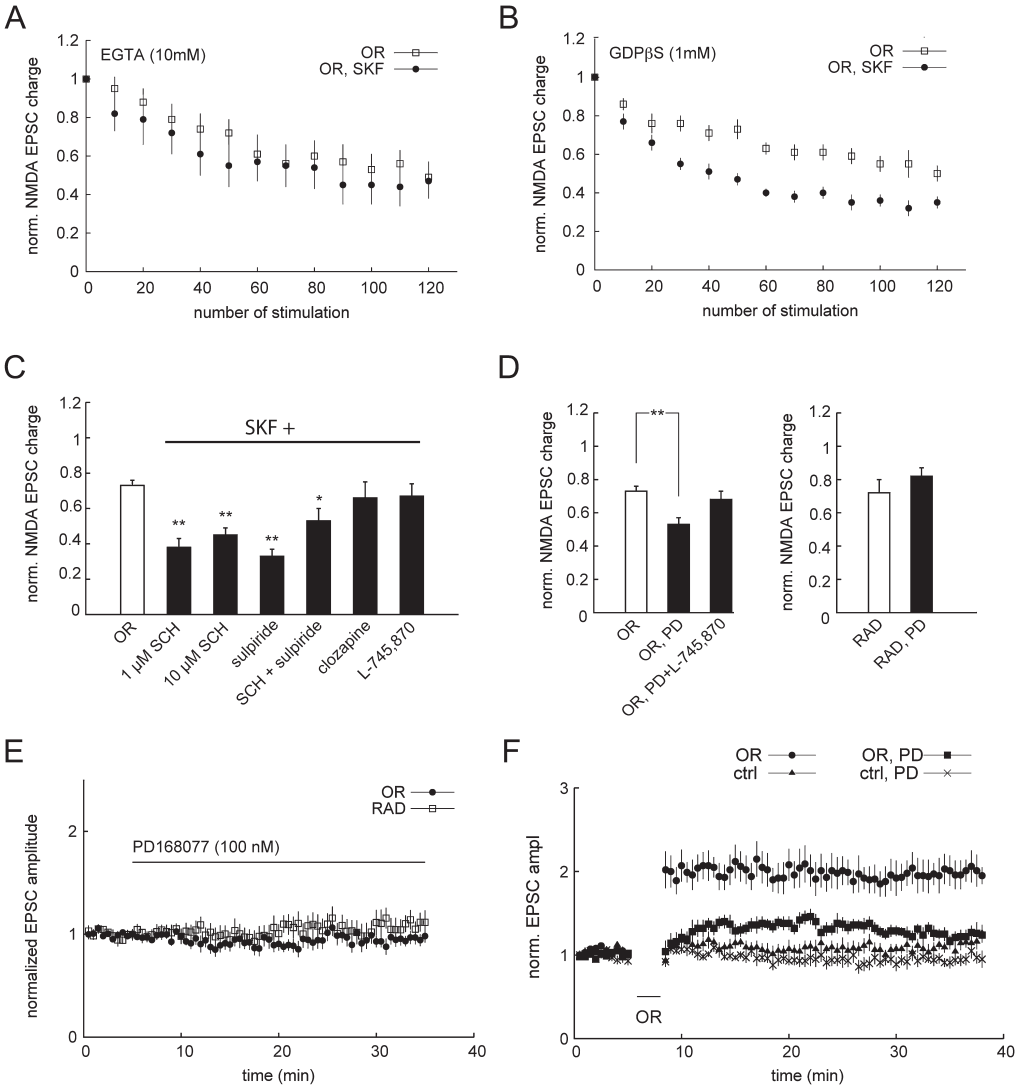

Figure 8. Effects of drugs chelating Ca^{2+}, blocking G-proteins or antagonizing dopamine receptors. One hundred and twenty LFS pairings were performed at +20 mV membrane potential during AMPAR blockade (NBQX, 5 μM). (*A*) EGTA (10 mM) in the patch pipette blocks the SKF38393-induced reduction in NMDAR-mediated charge transfer. Ten consecutive NMDA EPSCs were averaged and normalized to NMDA EPSCs evoked before at 0.05 Hz. (*B*) As in *A*, but with the G-protein blocker GDPβS (1 mM) present in the patch pipette. Note that GDPβS did not block the SKF38393-induced reduction in NMDA EPSC charge transfer. Data are shown as mean ± SEM. (*C*) Summary graph showing averaged charge transfer in OR in the presence of both 50 μM SKF38393 and dopamine receptor antagonists (SCH23390, 1 or 10 μM; sulpiride, 15 μM; SCH23390 and sulpiride, 1 and 10 μM; clozapine, 20 μM; L-745,870, 100 nM). (*D*) Summary graph showing averaged charge transfer in OR (left) and RAD (right) during LFS pairing at 0.67 Hz in control solution (open bar), in the presence of 100 nM PD168077 (filled bar) alone or together with L-745,870. Note the selective reduction of charge transfer in OR. (*E*) Normalized EPSC amplitudes from the OR and the RAD pathways during bath perfusion of 100 nM PD168077, relative to baseline, that is, absence of drug. (*F*) Normalized and pooled ($n = 6$) EPSC amplitudes evoked in OR and RAD without or with 100 nM PD168077 present in the whole-cell configuration at −70 mV. The time period of LFS pairing is indicated by the horizontal bar (OR). The respective unpaired control pathways are also shown. * and ** indicate $P < 0.05$ and $P < 0.01$, respectively. Data are shown as mean ± SEM.

Discussion

Here, we compared the effects of synthetic DA receptor ligands in stratum oriens (OR) and stratum radiatum (RAD) in the CA1 region of the dorsal hippocampus of 4-week-old mice. D4R activation selectively reduced early LTP in OR by reducing NMDAR-mediated charge transfer via an NR2B Ca^{2+}-dependent G-protein–independent mechanism.

Dopaminergic Input to the Hippocampal CA1 Region Differentially Modulates LTP

We observed intensively stained DAT-positive fibers in OR, a finding that is supported by the identification of dopaminergic fibers in rat and mouse hippocampus (Gasbarri et al. 1994; Gasbarri et al. 1997; Kwon et al. 2008). These findings may be consistent with a more pronounced dopaminergic innervation in OR than in RAD, which requires further investigation in the future. In the presence of the D1R/D5R agonist SKF38393 at a high (μM) concentration or in the presence of the D4R agonist PD168077 at a low (nM) concentration, we observed a pathway-specific reduction in the amount of LTP in OR. In field recordings, the reduction of the AMPA component developed gradually following the induction by HFS, whereas in whole-cell configuration, the synaptic efficacy was immediately reduced following LFS pairing (low-frequency synaptic stimulation paired with postsynaptic depolarization). This effect was in contrast to the lack of modulatory effects by SKF38393 in RAD.

Similar to the lateral amygdala (Bissiere et al. 2003), the dopaminergic gating of LTP in the temporoammonic (TA)–CA1 pathway in SLM has been ascribed to a diminished feed-forward inhibition (Ito and Schuman 2007), thus facilitating the LTP induction (Wigstrom and Gustafsson 1983). The reduced LTP we observed in OR in presence of SKF38393 was obtained while $GABA_A$ receptors were blocked with bicuculline, which suggests a different gating mechanism than the one mediated through inhibitory interneurons. Distinct mechanisms underlying the dopaminergic modulation of LTP induction and expression in SLM versus RAD/OR are also indicated by the fact that SKF38393 and dopamine itself reduced low-frequency activated synaptic responses in SLM (Otmakhova and Lisman 1999; Ito and Schuman 2007) but neither in RAD (Otmakhova and Lisman 1996; Mockett et al. 2004) nor in OR (our results).

Mechanism for Negative Dopaminergic LTP Modulation in OR

The major DA receptor signaling cascades are G-protein linked and activate or inhibit adenylate cyclase, thereby affecting cAMP production, the activity of PKA, cAMP-regulated DARPP-32, and voltage-gated Ca^{2+} channels (Seamans and Yang 2004). Alternative signaling cascades may involve interactions between D2-like DA receptors and the platelet-derived growth factor receptor beta (PDGFRbeta) (Kotecha et al. 2002) or direct protein–protein interactions between the intracellular C-termini of DA receptors and NMDARs. Interactions exist either between D1 and NR1 or NR2A (Lee et al. 2002) or between D2 and NR2B (Liu et al. 2006). These interactions most likely take place in postsynaptic membranes, where PDGFRbeta is expressed (Beazely et al. 2009) and DA receptors and NMDARs are known to colocalize (Hara and Pickel 2005). Thus, postsynaptic membranes provide the basis for functional interactions between dopaminergic and glutamatergic systems.

Our pharmacological analysis of NMDA EPSCs indicated that the augmented inactivation of NMDARs in OR is mediated through D4Rs, since the D4R antagonist L-745,870 prevented the SKF38393-induced NMDAR inactivation—a finding also supported by the experiments using clozapine. This possibility was strengthened by our demonstration that a D4R agonist (PD168077) also induced the pathway-specific NMDAR modulation in OR, an effect which was antagonized by the D4R antagonist L-745,870. Therefore, the D1R/D5R agonist SKF38393 at 50 μM is not D1 selective. Additionally, SKF38393 activated D4Rs, which modulated NMDA EPSCs in OR, whereas the binding of SKF38393 to D1Rs did not affect the inactivation of NMDA EPSCs for 2 reasons. 1) The rather selective D1R/D5R antagonist SCH23390 did not prevent the SKF38393 (50 μM)-induced NMDAR inactivation. 2) Lower concentrations of SKF38393 (10 and 20 μM) were insufficient to reduce the NMDA EPSC charge transfer in OR (data not shown). In contrast, a contribution of D1/D2 heterooligomers cannot be excluded (Hasbi et al. 2010) because the SKF38393-induced NMDAR inactivation was reduced by simultaneously antagonizing D1R/D5Rs (SCH23390) and D2-like DA receptors (sulpiride).

We employed NMDAR mutant mice in which either the NR2A or the NR2B alleles are inactive and demonstrated that NR2B- but not NR2A-containing NMDARs allowed the dopaminergic modulation in OR, that is, the reduced NMDAR-mediated postsynaptic charge transfer during LFS pairing and the consequent reduction in LTP magnitude. Because NR2A expression is substantial in 4 week-old wild-type mice, DA modulation in hippocampal synapses may embrace triheteromeric NR1/NR2A/NR2B receptors (Köhr 2006). These NMDAR subtypes comprise a notable fraction of the total NMDAR population based on biochemical analyses of whole hippocampus (Al-Hallaq et al. 2007) and on electrophysiological analyses of hippocampal CA1 synapses (Rauner and Köhr 2011). Our experiments, in which we applied a Ca^{2+} chelator or a G-protein inhibitor via the patch pipette intracellularly, indicated that the dopaminergic modulation of NMDA EPSCs in OR involves a postsynaptic mechanism that is Ca^{2+} dependent but G-protein independent. PDGFRbeta signaling may be one potential postsynaptic mechanism. Activation of PDGFRbeta in hippocampal slices by the D2-like agonist quinpirole, known as transactivation, was reported to enhance calmodulin- and Ca^{2+}-dependent inactivation of NMDARs (Kotecha et al. 2002). Interestingly, PDGFRbeta activation by growth factor preferentially inhibited NR2B-containing NMDARs in isolated CA1 neurons (Beazely et al. 2009). Since quinpirole did not augment the NMDAR inactivation in OR (data not shown), we favor the possibility that a direct protein–protein interaction between D2R and NR2B subunits might underlie the dopaminergic modulation of LTP in OR. Direct D2R–NR2B interaction has been reported to be enhanced in response to cocaine, disrupting the association between CaMKII and NR2B, and reducing NMDA currents in dissociated striatal neurons (Liu et al. 2006). Consistently, transgenic mice with a disrupted CaMKII–NR2B interaction are impaired in hippocampal LTP and spatial learning (Zhou et al. 2007). A similar CaMKII–NR2B disruption may occur during the dopaminergic modulation of LTP that we describe in OR, which will be of interest for future studies.

Dopaminergic Modulation of Hippocampal Learning and Memory

The DA contribution to hippocampus-dependent learning and memory is incompletely understood. Recent studies have focused on the D1R/D5R-mediated modulation of hippocampus-dependent learning (Tran et al. 2008; Bethus et al. 2010; Nai et al. 2010; Ortiz et al. 2010; Xing et al. 2010). Our results add new dimensions, including D4R contribution in stratum oriens. Beside OR, SLM could be another distinct CA1 subregion for dopaminergic modulation of learning and memory, as previously implied in plasticity studies (Otmakhova and Lisman 1999; Ito and Schuman 2007). Thus, the future challenge will be to understand the function of the differential DA modulation in OR and SLM during hippocampal learning and memory. These hippocampal considerations will also be interesting because of the recently reported dopaminergic modulation of synapses at the cortical input and the subicular output (Roggenhofer et al. 2010; Mu et al. 2011).

Stratum Oriens as Functional Link in Cognitive Disorders?

Both dopaminergic hyperfunction in VTA and NMDAR hypofunction in the hippocampus have been implicated in the pathophysiology of schizophrenia (reviewed in Lisman et al. 2008). Whether one neurotransmitter system causes the alterations in the other or whether they coexist without causal relation is unknown. Aberrant hippocampal activity can lead to

abnormal firing of DA neurons in the VTA (Floresco et al. 2003; Lodge and Grace 2007). However, local effects may play a role, as, for example, stimulation of dopamine release within the hippocampus by neuregulin-1 is sufficient to suppress LTP without VTA involvement (Kwon et al. 2008).

Here, we suggest that stratum oriens could be an overlooked link between dopaminergic and glutamatergic systems underlying cognition. Malfunctions in either system or in their interactions may contribute to the deficits observed in a variety of mental disorders (Heckers et al. 1998). For instance, DA neurons in the VTA are highly active in schizophrenia, leading to increased DA release in target regions. In OR, the subsequent activation of DA receptors on basal dendrites of CA1 neurons inactivates NR2B-containing NMDARs in a Ca^{2+}-dependent manner, impairing LTP as a consequence. This mechanism links DA hyperfunction in VTA and NMDAR hypofunction in the hippocampus. Thus, the severity of symptoms of mental disorders may depend on dysfunctions in stratum oriens of the dopaminergic and glutamatergic neurotransmitter pathways, and consideration could be beneficial therapeutically.

Funding

Letten Foundation (to V.J. and O.H.).

Notes

We thank Dr M. Mishina (University of Tokyo) for providing *NR2A*$^{-/-}$ mice, Dr H. Monyer (University of Heidelberg) for *NR2B*$^{\Delta Fb}$ mice, Dr S. Berberich and A. K. Lee for valuable comments, and Dr P. H. Seeburg for generous support. *Conflict of Interest* : None declared.

References

Al-Hallaq RA, Conrads TP, Veenstra TD, Wenthold RJ. 2007. NMDA di-heteromeric receptor populations and associated proteins in rat hippocampus. J Neurosci. 27:8334–8343.

Beazely MA, Lim A, Li H, Trepanier C, Chen X, Sidhu B, Macdonald JF. 2009. Platelet-derived growth factor selectively inhibits NR2B-containing N-methyl-D-aspartate receptors in CA1 hippocampal neurons. J Biol Chem. 284:8054–8063.

Berberich S, Jensen V, Hvalby O, Seeburg PH, Köhr G. 2007. The role of NMDAR subtypes and charge transfer during hippocampal LTP induction. Neuropharmacology. 52:77–86.

Berberich S, Punnakkal P, Jensen V, Pawlak V, Seeburg PH, Hvalby O, Köhr G. 2005. Lack of NMDA receptor subtype selectivity for hippocampal long-term potentiation. J Neurosci. 25:6907–6910.

Bethus I, Tse D, Morris RG. 2010. Dopamine and memory: modulation of the persistence of memory for novel hippocampal NMDA receptor-dependent paired associates. J Neurosci. 30:1610–1618.

Bissiere S, Humeau Y, Luthi A. 2003. Dopamine gates LTP induction in lateral amygdala by suppressing feedforward inhibition. Nat Neurosci. 6:587–592.

Chen HX, Otmakhov N, Lisman J. 1999. Requirements for LTP induction by pairing in hippocampal CA1 pyramidal cells. J Neurophysiol. 82:526–532.

Cragg SJ, Rice ME. 2004. DAncing past the DAT at a DA synapse. Trends Neurosci. 27:270–277.

Floresco SB, West AR, Ash B, Moore H, Grace AA. 2003. Afferent modulation of dopamine neuron firing differentially regulates tonic and phasic dopamine transmission. Nat Neurosci. 6:968–973.

Frey U, Matthies H, Reymann KG. 1991. The effect of dopaminergic D1 receptor blockade during tetanization on the expression of long-term potentiation in the rat CA1 region in vitro. Neurosci Lett. 129:111–114.

Gasbarri A, Packard MG, Campana E, Pacitti C. 1994. Anterograde and retrograde tracing of projections from the ventral tegmental area to the hippocampal formation in the rat. Brain Res Bull. 33:445–452.

Gasbarri A, Sulli A, Packard MG. 1997. The dopaminergic mesencephalic projections to the hippocampal formation in the rat. Prog Neuropsychopharmacol Biol Psychiatry. 21:1–22.

Granado N, Ortiz O, Suarez LM, Martin ED, Cena V, Solis JM, Moratalla R. 2008. D1 but not D5 dopamine receptors are critical for LTP, spatial learning, and LTP-induced arc and zif268 expression in the hippocampus. Cereb Cortex. 18:1–12.

Greene R. 2001. Circuit analysis of NMDAR hypofunction in the hippocampus, in vitro, and psychosis of schizophrenia. Hippocampus. 11:569–577.

Hara Y, Pickel VM. 2005. Overlapping intracellular and differential synaptic distributions of dopamine D1 and glutamate N-methyl-D-aspartate receptors in rat nucleus accumbens. J Comp Neurol. 492:442–455.

Hasbi A, O'Dowd BF, George SR. 2010. Heteromerization of dopamine D2 receptors with dopamine D1 or D5 receptors generates intracellular calcium signaling by different mechanisms. Curr Opin Pharmacol. 10:93–99.

Heckers S, Rauch SL, Goff D, Savage CR, Schacter DL, Fischman AJ, Alpert NM. 1998. Impaired recruitment of the hippocampus during conscious recollection in schizophrenia. Nat Neurosci. 1:318–323.

Huang YY, Kandel ER. 1995. D1/D5 receptor agonists induce a protein synthesis-dependent late potentiation in the CA1 region of the hippocampus. Proc Natl Acad Sci U S A. 92:2446–2450.

Ito HT, Schuman EM. 2007. Frequency-dependent gating of synaptic transmission and plasticity by dopamine. Front Neural Circuits. 1:1.

Köhr G. 2006. NMDA receptor function: subunit composition versus spatial distribution. Cell Tissue Res. 326:439–446.

Köhr G, Jensen V, Koester HJ, Mihaljevic AL, Utvik JK, Kvello A, Ottersen OP, Seeburg PH, Sprengel R, Hvalby O. 2003. Intracellular domains of NMDA receptor subtypes are determinants for long-term potentiation induction. J Neurosci. 23:10791–10799.

Kotecha SA, Oak JN, Jackson MF, Perez Y, Orser BA, Van Tol HH, MacDonald JF. 2002. A D2 class dopamine receptor transactivates a receptor tyrosine kinase to inhibit NMDA receptor transmission. Neuron. 35:1111–1122.

Krupp JJ, Vissel B, Thomas CG, Heinemann SF, Westbrook GL. 1999. Interactions of calmodulin and alpha-actinin with the NR1 subunit modulate Ca^{2+}-dependent inactivation of NMDA receptors. J Neurosci. 19:1165–1178.

Kwon OB, Paredes D, Gonzalez CM, Neddens J, Hernandez L, Vullhorst D, Buonanno A. 2008. Neuregulin-1 regulates LTP at CA1 hippocampal synapses through activation of dopamine D4 receptors. Proc Natl Acad Sci U S A. 105:15587–15592.

Lee FJ, Xue S, Pei L, Vukusic B, Chery N, Wang Y, Wang YT, Niznik HB, Yu XM, Liu F. 2002. Dual regulation of NMDA receptor functions by direct protein-protein interactions with the dopamine D1 receptor. Cell. 111:219–230.

Lemon N, Manahan-Vaughan D. 2006. Dopamine D1/D5 receptors gate the acquisition of novel information through hippocampal long-term potentiation and long-term depression. J Neurosci. 26:7723–7729.

Lewis DA, Lieberman JA. 2000. Catching up on schizophrenia: natural history and neurobiology. Neuron. 28:325–334.

Lisman JE, Coyle JT, Green RW, Javitt DC, Benes FM, Heckers S, Grace AA. 2008. Circuit-based framework for understanding neurotransmitter and risk gene interactions in schizophrenia. Trends Neurosci. 31:234–242.

Lisman JE, Grace AA. 2005. The hippocampal-VTA loop: controlling the entry of information into long-term memory. Neuron. 46:703–713.

Liu XY, Chu XP, Mao LM, Wang M, Lan HX, Li MH, Zhang GC, Parelkar NK, Fibuch EE, Haines M, et al. 2006. Modulation of D2R-NR2B interactions in response to cocaine. Neuron. 52:897–909.

Lodge DJ, Grace AA. 2007. Aberrant hippocampal activity underlies the dopamine dysregulation in an animal model of schizophrenia. J Neurosci. 27:11424–11430.

Malenka RC, Bear MF. 2004. LTP and LTD: an embarrassment of riches. Neuron. 44:5–21.

Meltzer HY. 1995. Role of serotonin in the action of atypical antipsychotic drugs. Clin Neurosci. 3:64–75.

Mockett BG, Brooks WM, Tate WP, Abraham WC. 2004. Dopamine D1/D5 receptor activation fails to initiate an activity-independent late-phase LTP in rat hippocampus. Brain Res. 1021:92–100.
Mu Y, Zhao C, Gage FH. 2011. Dopaminergic modulation of cortical inputs during maturation of adult-born dentate granule cells. J Neurosci. 31:4113–4123.
Nai Q, Li S, Wang SH, Liu J, Lee FJ, Frankland PW, Liu F. 2010. Uncoupling the D1-N-methyl-D-aspartate (NMDA) receptor complex promotes NMDA-dependent long-term potentiation and working memory. Biol Psychiatry. 67:246–254.
Navakkode S, Sajikumar S, Frey JU. 2007. Synergistic requirements for the induction of dopaminergic D1/D5-receptor-mediated LTP in hippocampal slices of rat CA1 in vitro. Neuropharmacology. 52:1547–1554.
Novak A, Guo C, Yang W, Nagy A, Lobe CG. 2000. Z/EG, a double reporter mouse line that expresses enhanced green fluorescent protein upon Cre-mediated excision. Genesis. 28:147–155.
O'Carroll CM, Martin SJ, Sandin J, Frenguelli B, Morris RG. 2006. Dopaminergic modulation of the persistence of one-trial hippocampus-dependent memory. Learn Mem. 13:760–769.
Ortiz O, Delgado-Garcia JM, Espadas I, Bahi A, Trullas R, Dreyer JL, Gruart A, Moratalla R. 2010. Associative learning and CA3-CA1 synaptic plasticity are impaired in D1R null, Drd1a−/− mice and in hippocampal siRNA silenced Drd1a mice. J Neurosci. 30:12288–12300.
Otmakhova NA, Lisman JE. 1996. D1/D5 dopamine receptor activation increases the magnitude of early long-term potentiation at CA1 hippocampal synapses. J Neurosci. 16:7478–7486.
Otmakhova NA, Lisman JE. 1999. Dopamine selectively inhibits the direct cortical pathway to the CA1 hippocampal region. J Neurosci. 19:1437–1445.
Parlato R, Rieker C, Turiault M, Tronche F, Schutz G. 2006. Survival of DA neurons is independent of CREM upregulation in absence of CREB. Genesis. 44:454–464.
Rauner C, Köhr G. 2011. Triheteromeric NR1/NR2A/NR2B receptors constitute the major N-methyl-D-aspartate receptor population in adult hippocampal synapses. J Biol Chem. 286:7558–7566.
Roggenhofer E, Fidzinski P, Bartsch J, Kurz F, Shor O, Behr J. 2010. Activation of dopamine D1/D5 receptors facilitates the induction of presynaptic long-term potentiation at hippocampal output synapses. Eur J Neurosci. 32:598–605.
Romo-Parra H, Aceves J, Gutierrez R. 2005. Tonic modulation of inhibition by dopamine D4 receptors in the rat hippocampus. Hippocampus. 15:254–259.
Sakimura K, Kutsuwada T, Ito I, Manabe T, Takayama C, Kushiya E, Yagi T, Aizawa S, Inoue Y, Sugiyama H, et al. 1995. Reduced hippocampal LTP and spatial learning in mice lacking NMDA receptor epsilon 1 subunit. Nature. 373:151–155.
Seeman P, Van Tol HH. 1994. Dopamine receptor pharmacology. Trends Pharmacol Sci. 15:264–270.
Seamans JK, Yang CR. 2004. The principal features and mechanisms of dopamine modulation in the prefrontal cortex. Prog Neurobiol. 74:1–58.
Stramiello M, Wagner JJ. 2008. D1/5 receptor-mediated enhancement of LTP requires PKA, Src family kinases, and NR2B-containing NMDARs. Neuropharmacology. 55:871–877.
Stramiello M, Wagner JJ. 2010. Cocaine enhancement of long-term potentiation in the CA1 region of rat hippocampus: lamina-specific mechanisms of action. Synapse. 64:644–648.
Svensson TH. 2003. Alpha-adrenoceptor modulation hypothesis of antipsychotic atypicality. Prog Neuropsychopharmacol Biol Psychiatry. 27:1145–1158.
Swanson-Park JL, Coussens CM, Mason-Parker SE, Raymond CR, Hargreaves EL, Dragunow M, Cohen AS, Abraham WC. 1999. A double dissociation within the hippocampus of dopamine D1/D5 receptor and beta-adrenergic receptor contributions to the persistence of long-term potentiation. Neuroscience. 92:485–497.
Swant J, Wagner JJ. 2006. Dopamine transporter blockade increases LTP in the CA1 region of the rat hippocampus via activation of the D3 dopamine receptor. Learn Mem. 13:161–167.
Tarazi FI, Baldessarini RJ. 2000. Comparative postnatal development of dopamine D(1), D(2) and D(4) receptors in rat forebrain. Int J Dev Neurosci. 18:29–37.
Tran AH, Uwano T, Kimura T, Hori E, Katsuki M, Nishijo H, Ono T. 2008. Dopamine D1 receptor modulates hippocampal representation plasticity to spatial novelty. J Neurosci. 28:13390–13400.
Varela JA, Hirsch SJ, Chapman D, Leverich LS, Greene RW. 2009. D1/D5 modulation of synaptic NMDA receptor currents. J Neurosci. 29:3109–3119.
Verney C, Baulac M, Berger B, Alvarez C, Vigny A, Helle KB. 1985. Morphological evidence for a dopaminergic terminal field in the hippocampal formation of young and adult rat. Neuroscience. 14:1039–1052.
von Engelhardt J, Doganci B, Jensen V, Hvalby O, Gongrich C, Taylor A, Barkus C, Sanderson DJ, Rawlins JN, Seeburg PH, et al. 2008. Contribution of hippocampal and extra-hippocampal NR2B-containing NMDA receptors to performance on spatial learning tasks. Neuron. 60:846–860.
Wigstrom H, Gustafsson B. 1983. Facilitated induction of hippocampal long-lasting potentiation during blockade of inhibition. Nature. 301:603–604.
Winterer G, Weinberger DR. 2004. Genes, dopamine and cortical signal-to-noise ratio in schizophrenia. Trends Neurosci. 27:683–690.
Xing B, Kong H, Meng X, Wei SG, Xu M, Li SB. 2010. Dopamine D1 but not D3 receptor is critical for spatial learning and related signaling in the hippocampus. Neuroscience. 169:1511–1519.
Zhang S, Ehlers MD, Bernhardt JP, Su CT, Huganir RL. 1998. Calmodulin mediates calcium-dependent inactivation of N-methyl-D-aspartate receptors. Neuron. 21:443–453.
Zhou Y, Takahashi E, Li W, Halt A, Wiltgen B, Ehninger D, Li GD, Hell JW, Kennedy MB, Silva AJ. 2007. Interactions between the NR2B receptor and CaMKII modulate synaptic plasticity and spatial learning. J Neurosci. 27:13843–13853.